Available online at www.sciencedirect.com
SCIENCE DIRECT
Journal of the European Ceramic Society 26 (2006) 1619–1628
www.elsevier.com/locate/jeurceramsoc

Inhibition of abnormal grain growth in $BaTiO_3$ by addition of Al_2O_3

John G. Fisher [a], Byong-Ki Lee [b], Si-Young Choi [a], Seong-Min Wang [a], Suk-Joong L. Kang [a,*]

[a] *Department of Materials Science and Engineering, Korea Advanced Institute of Science and Technology, 373-1 Kusong-dong, Yusong-gu, Daejon 305-701, Republic of Korea*
[b] *Memory Research and Development Division, Hynix Electronics Industry Company Ltd., Ichon, Kyoungki 467-860, Republic of Korea*

Received 17 September 2004; received in revised form 24 February 2005; accepted 5 March 2005
Available online 11 April 2005

Abstract

The effect of additions of up to 1 mol% Al_2O_3 on abnormal grain growth in $BaTiO_3$ samples sintered at 1200 and 1250 °C has been studied. Samples with and without additions of 0.4 mol% TiO_2 were prepared. For the samples without added TiO_2, addition of 0.1 mol% Al_2O_3 increases the number density of abnormal grains, with further additions reducing the number density. The initial increase in number density is caused by Al_2O_3 forming a solid solution with $BaTiO_3$ and releasing TiO_2 to the grain boundaries. This excess TiO_2 then reacts with $BaTiO_3$ to form $Ba_6Ti_{17}O_{40}$, which promotes {1 1 1} twin formation and abnormal grain growth. Further additions of Al_2O_3 react with $BaTiO_3$, $Ba_6Ti_{17}O_{40}$ and excess TiO_2 to form $Ba_4Al_2Ti_{10}O_{27}$ and $BaAl_2O_4$ second phases, neither of which are growth sites for abnormal grains. For the samples with added TiO_2, addition of Al_2O_3 decreases the number of abnormal grains due to the Al_2O_3 reacting with the excess TiO_2 and $BaTiO_3$ to form $Ba_4Al_2Ti_{10}O_{27}$ and $BaAl_2O_4$ instead of $Ba_6Ti_{17}O_{40}$.
© 2005 Elsevier Ltd. All rights reserved.

Keywords: $BaTiO_3$ and titanates; Al_2O_3; Interfaces; Abnormal grain growth

1. Introduction

$BaTiO_3$ is an important dielectric ceramic with many uses such as capacitors and positive temperature coefficient of resistance (PTCR) materials. In these applications, control of the microstructure is necessary to optimize properties. The microstructure is dependant on processing factors such as sintering temperature and the presence of dopants or impurities. The $BaTiO_3$–TiO_2 system has a $BaTiO_3$–$Ba_6Ti_{17}O_{40}$ eutectic at 1332 °C.[1] When $BaTiO_3$ is sintered at temperatures above this eutectic point primary abnormal grain growth (PAGG) takes place.[2,3] Abnormally large grains nucleate and grow, consuming the fine matrix grains. This abnormal grain growth (AGG) is very rapid and the original fine-grained matrix can be completely replaced by coarse grains after 1 h of sintering at 1355 °C.[4] After PAGG is completed the microstructure appears to have a log normal size distribution. If the sintering temperature is between 1360 and 1370 °C, then secondary abnormal grain growth (SAGG) can follow PAGG: some of the coarse primary grains begin to grow rapidly and consume the other primary grains.[4] This behaviour is linked to the presence of (1 1 1) twins.[4,5]

At temperatures below the eutectic, abnormal grain growth takes place.[3,6–8] Some of the matrix grains grow to a large size, forming a bimodal microstructure of fine matrix grains and large abnormal grains. Although AGG can be extensive in samples sintered for long periods below the eutectic temperature, complete consumption of the original matrix grains does not take place.

Both PAGG and AGG are affected by dopants. The eutectic point mentioned above can be lowered to ~1250 °C by the addition of Al_2O_3–SiO_2–TiO_2,[9] leading to PAGG at lower sintering temperatures.[2] When $BaTiO_3$ is doped with donor concentrations exceeding 0.3–0.5 at.% and sintered above the eutectic temperature, PAGG does not take place.

* Corresponding author. Tel.: +82 42 869 4113; fax: +82 42 869 8920.
E-mail address: sjkang@kaist.ac.kr (S.-J.L. Kang).

0955-2219/$ – see front matter © 2005 Elsevier Ltd. All rights reserved.
doi:10.1016/j.jeurceramsoc.2005.03.234

This is known as the grain growth anomaly[10] or grain growth inhibition threshold.[11] Both A- and B-site donors effectively suppress PAGG.[12]

Below the eutectic, different additives can promote or suppress AGG, each according to its own mechanism. AGG is promoted by excess TiO_2.[13] TiO_2 reacts with $BaTiO_3$ to form $Ba_6Ti_{17}O_{40}$, which acts as a nucleation site for {1 1 1} twins.[13] These twins provide growth sites for abnormal grains by the twin-plane re-entrant edge mechanism.[5,14,15] For {1 1 1} twins to nucleate, the $Ba_6Ti_{17}O_{40}$ phase must be faceted (atomically smooth).[13,16] Excess TiO_2 is often added to $BaTiO_3$ as a sintering aid. If the excess TiO_2 is decreased to zero, then AGG is eliminated and normal grain growth occurs.[17] La_2O_3 has been found to suppress AGG below the eutectic temperature by the formation of $La_2Ti_2O_7$ precipitates which scavenge excess TiO_2.[11] ZnO suppresses AGG by segregation at the grain boundaries which decreases the grain boundary mobility.[18]

Although the effect of donor dopants on the grain growth of $BaTiO_3$ has been extensively studied, the effect of acceptor dopants is less well known. Acceptor dopants are often present as impurities and are sometimes added as sintering aids[19] and to modify the PTCR properties of $BaTiO_3$.[19,20] Na_2O inhibits AGG in Ti-excess $BaTiO_3$ sintered at 1215 °C by the formation of Na_4TiO_4 precipitates, which scavenge excess TiO_2.[21] Čeh and Kolar[22] found that CaO caused a decrease in primary abnormal grain size in samples sintered at 1450 °C and attributed this to the formation of $Ba_3Ca_2Ti_2O_9$ at the grain boundaries. However, as Ca^{2+} substituted for Ti^{4+} in their work, the reduction in grain size may have been due to the excess Ti rather than the second phase.[3]

Al_2O_3 has been added to $BaTiO_3$ as an acceptor dopant[23,24] and as a sintering aid in conjunction with SiO_2 and TiO_2.[25,26] Addition of Al_2O_3–SiO_2–TiO_2 has been found to reduce the primary abnormal grain size, leading to a finer microstructure,[2] and to suppress AGG.[25] Although the effect of Al_2O_3–SiO_2–TiO_2 addition on microstructure development is well known, the effect of Al_2O_3 by itself has not been studied extensively. Cheng[26] found that addition of 0.3 mol% Al_2O_3 to SiO_2-doped $BaTiO_3$ reduced the average grain size of samples sintered at 1350 °C and improved uniformity. On the other hand, Al-Allak et al.[24] found that addition of 0.55 mol% Al_2O_3 to $BaTiO_3$ (with small amounts of SiO_2 and TiO_2 added as sintering aids) caused an increase in average grain size at sintering temperatures between 1260 and 1400 °C. Addition of Al_2O_3 also caused the grain size distribution to widen, although AGG was absent in the samples. In both these works, SiO_2 and TiO_2 were added in addition to Al_2O_3.

Adding combinations of Al_2O_3, SiO_2 and TiO_2 makes it difficult to determine the effect that each separate additive has on abnormal grain growth behaviour. In the present investigation, we have therefore, studied the effect of Al_2O_3 addition alone on abnormal grain growth in $BaTiO_3$. The effect of Al_2O_3 additions of up to 1 mol% on the AGG behaviour of $BaTiO_3$ sintered at temperatures of 1200 and 1250 °C is described. TiO_2 is often added to $BaTiO_3$ as a sintering aid and so the effect of adding both Al_2O_3 and TiO_2 has also been studied. The AGG behaviour of the Al_2O_3-doped samples can be explained by considering the effect of second phases.

2. Experimental

$BaTiO_3$ powders were prepared from Fuji Titanium HPBT-1 $BaTiO_3$, Aldrich TiO_2 and Sumitomo AKP–50 Al_2O_3. Manufacturers' analyses of the powders are listed in Table 1. The Ba/Ti ratio of the $BaTiO_3$ powder is 0.997, i.e. there is a slight Ti excess. Two series of powders were prepared. The first series (series A) was doped with Al_2O_3 only. Powders were prepared with additions of 0, 0.1, 0.2, 0.5 and 1.0 mol% Al_2O_3. The second series (series T) was doped with 0.4 mol% TiO_2 in addition to Al_2O_3. Powders were prepared with additions of 0, 0.1, 0.5 and 1.0 mol% Al_2O_3. The powders were ball milled in ethanol in polypropylene jars using ZrO_2 milling media. After milling, the slurries were dried, crushed and passed through a 150 μm sieve. Samples 9 mm in diameter and 4 mm thick were prepared by cold isostatic pressing at 200 MPa. Samples were placed on $BaTiO_3$ spacers in an alumina crucible and sintered in an alumina tube furnace. Samples were sintered at 1200 and 1250 °C for 10 or 100 h. Samples were pushed into or pulled out of the furnace over a period of 1 h. The heating and cooling rate was ~20 °C min^{-1}.

Samples for optical microscopy and SEM were sectioned, polished to a 0.25 μm finish and etched in a solution of 1 vol.% HF–4 vol.% HCl–95 vol.% distilled H_2O for ~5 s. Abnormal grain number density was measured from optical micrographs (Model DMLM, Leica Microsystems, Wetzlar, Germany). For each sample, the average number density and standard deviation was measured from 6 to 10 micrographs depending on the sample. Samples for SEM were gold coated and viewed in a Model XL 30 S FEG SEM (Philips, Eindhoven, Netherlands). The matrix grain size was measured using an image analyzing program (Matrox Inspector

Table 1
Manufacturers' analyses of powders

Powder	Powder size (μm)	Purity (wt.%)	Impurities
$BaTiO_3$	0.65	99.8	Ba/Ti mol ratio: 0.997 0.001 wt.% Fe_2O_3 0.002 wt.% Na_2O <0.1 wt.% SrO <0.05 wt.% Al_2O_3 <0.05 wt.% SiO_2
TiO_2	0.3	>99.9	
Al_2O_3	0.1–0.3	>99.99	<20 ppm Fe_2O_3 <10 ppm Na_2O <25 ppm Si <10 ppm Cu <10 ppm Mg

2.1, Matrox Electronic Systems Ltd., Dorval, Canada) and divided by 0.76 to determine the 3D grain size.[27] For wavelength dispersive spectroscopy (WDS), samples were polished and etched as above, carbon coated, and viewed in a Model 515 SEM (Philips, Eindhoven, Netherlands). Samples were prepared for transmission electron microscopy (TEM) by the standard method of sectioning, grinding, dimpling and ion beam milling. Samples were viewed in a JEM-3010 (JEOL, Tokyo, Japan) TEM at 300 kV.

Samples for optical and scanning electron microscopy (SEM) were heat-treated in flowing H_2 at 900 °C. This treatment stabilises the cubic phase at room temperature, removes the domain structure and makes the {1 1 1} twins more visible.[28] Samples for WDS and TEM did not receive this H_2 heat treatment.

3. Results

Fig. 1 shows optical micrographs of series A samples that have been sintered at 1250 °C for 100 h. Fig. 1(a) shows a sample with 0 mol% Al_2O_3. Abnormal grain growth has occurred throughout the sample, leading to a bimodal microstructure of fine matrix grains and large abnormal grains up to 200 μm in diameter. The abnormal grains are polyhedral with faceted boundaries. {1 1 1} single and double twins (marked with arrows) are present in some of the abnormal grains but do not appear to affect the growth direction of the grains. Abnormal grains tend to congregate in clusters, although isolated abnormal grains are present. These clusters often have a 'rosette' appearance, with small abnormal grains in the centre of the cluster surrounded by larger abnormal grains.

Addition of 0.1 mol% Al_2O_3 causes an increase in the number of abnormal grains (Fig. 1(b)). The abnormal grains are reduced in size, the maximum size being ~100 μm, but their shape remains unchanged. Likewise, twinning is present in some of the grains and abnormal grains still cluster together. Addition of 0.5 mol% Al_2O_3 causes a large decrease in the number of abnormal grains (Fig. 1(c)). The maximum grain size of the abnormal grains increases to 200 μm and their average size increases. In the sample with 1.0 mol% Al_2O_3 AGG is almost completely eliminated (Fig. 1(d)), the abnormal grains in the micrograph being the only ones visible in the plane of polish of this sample.

Fig. 2 shows optical micrographs of series T samples. Fig. 2(a) shows the sample with 0 mol% Al_2O_3. AGG has occurred to a much greater degree in this sample than in the equivalent series A sample with no added TiO_2 (Fig. 1(a)). The original fine-grained matrix has been almost completely consumed by abnormal grains, with matrix grains remaining in the gaps between abnormal grains. Both polyhedral

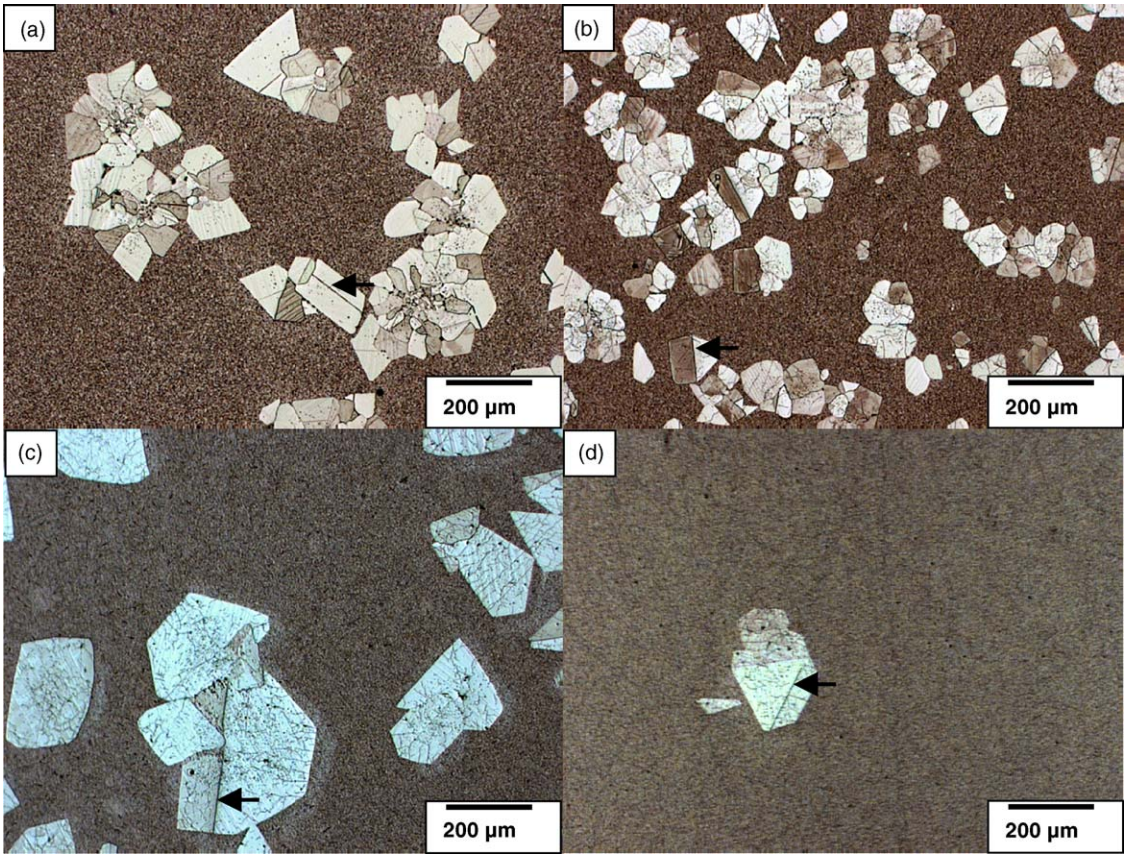

Fig. 1. $BaTiO_3$ samples doped with: (a) 0; (b) 0.1; (c) 0.5 and (d) 1.0 mol% Al_2O_3 sintered at 1250 °C for 100 h.

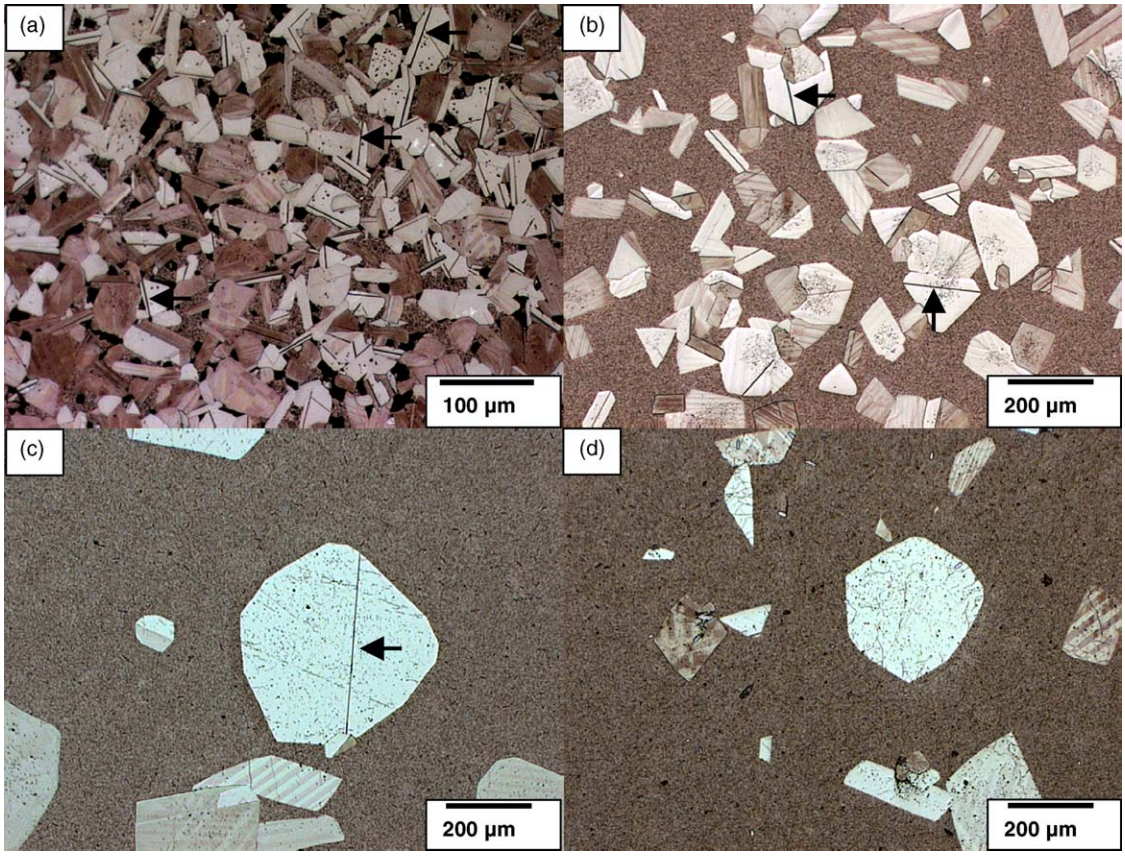

Fig. 2. $BaTiO_3$ 0.4 mol% TiO_2 samples doped with: (a) 0; (b) 0.1; (c) 0.5 and (d) 1.0 mol% Al_2O_3 sintered at 1250 °C for 100 h.

and elongated abnormal grains are present. Single and double {1 1 1} twins are present in many of the abnormal grains (marked with arrows). In the elongated abnormal grains, the {1 1 1} twin runs parallel to the long face of the grain. In some of the polyhedral grains, two twins intersecting each other at an angle are visible.

Unlike the series A samples, addition of Al_2O_3 immediately causes a sharp decrease in the number of abnormal grains in the series T samples (Fig. 2(b)). The size of the abnormal grains increases and the shape of the abnormal grains changes from both elongated and polyhedral to largely polyhedral. Further additions of Al_2O_3 cause the number of abnormal grains to decrease further, with the number levelling out at 0.5 mol% Al_2O_3.

The samples of both series sintered at 1250 °C for 10 h follow the same patterns as above, although the extent of AGG is reduced. The samples of both series sintered at 1200 °C for 10 h show very little or no abnormal grain growth. The samples of both series sintered at 1200 °C for 100 h show appreciable abnormal grain growth. Abnormal grains in these samples are much smaller than abnormal grains in the corresponding samples sintered at 1250 °C. Abnormal grains in the samples sintered at 1200 °C are faceted and elongated. All the abnormal grains have single or double {1 1 1} twins running parallel to the long face of the grain. Some abnormal grains are polyhedral, with two {1 1 1} twins intersecting each other at an angle. The series A samples sintered at 1200 °C for 100 h display similar behaviour to the samples sintered at 1250 °C: addition of 0.1 mol% Al_2O_3 causes an increase in the number of abnormal grains, with further additions causing a decrease. The series T samples sintered at 1200 °C for 100 h also display similar behaviour to the samples sintered at 1250 °C: addition of Al_2O_3 causes a decrease in the number of abnormal grains. However, the shape of the abnormal grains in the series T samples sintered at 1200 °C does not change from elongated to polyhedral with addition of Al_2O_3. Representative micrographs of samples sintered at 1200 °C are shown in Fig. 3.

The effect of Al_2O_3 on the number density of abnormal grains in samples sintered for 100 h is shown in Fig. 4. For the series A samples, addition of 0.1 mol% Al_2O_3 causes a large increase in the number density of abnormal grains. Further addition of Al_2O_3 causes a rapid drop in the number density of abnormal grains. For the series T samples, addition of Al_2O_3 causes a sharp decrease in the number density of abnormal grains, with the number density levelling out at 0.5 mol% Al_2O_3. Al_2O_3 doping has the same effect on the samples regardless of sintering temperature. In the series A samples the sample doped with 0.1 mol% Al_2O_3 shows a higher abnormal grain number density when sintered at 1200 °C than when sintered at 1250 °C. In the series T samples, the sample without Al_2O_3 doping shows a higher abnormal grain number

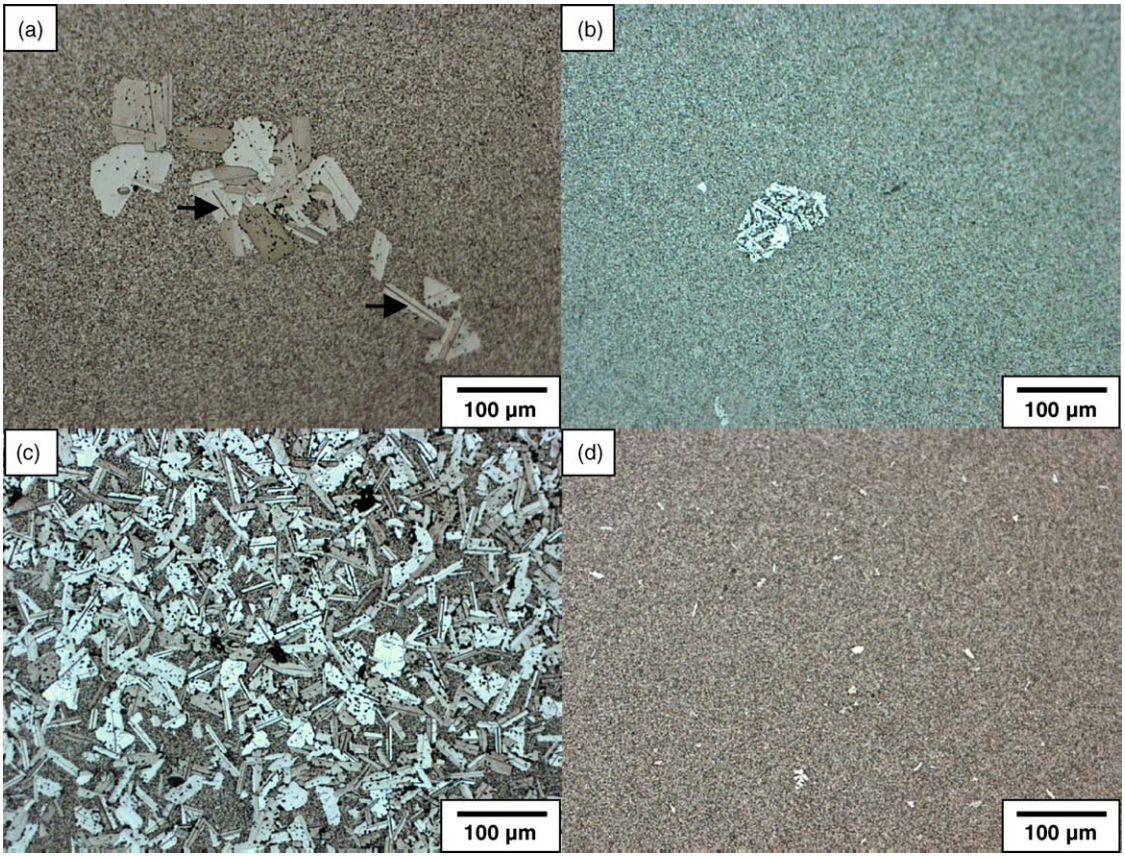

Fig. 3. $BaTiO_3$ samples doped with: (a) 0 mol% Al_2O_3; (b) 0.5 mol% Al_2O_3; (c) 0.4 mol% TiO_2; (d) 0.4 mol% TiO_2 0.5 mol% Al_2O_3 sintered at 1200 °C for 100 h.

density when sintered at 1200 °C than when sintered at 1250 °C.

Fig. 5 shows TEM micrographs of matrix grains from series A samples. Micro-faceting (marked by arrows) is visible in all of the samples, irrespective of Al_2O_3 content. Addition of Al_2O_3 has not caused a roughening transition in $BaTiO_3$. Also visible in Fig. 5(c) is an amorphous pocket at a triple junction (marked with a dotted circle).

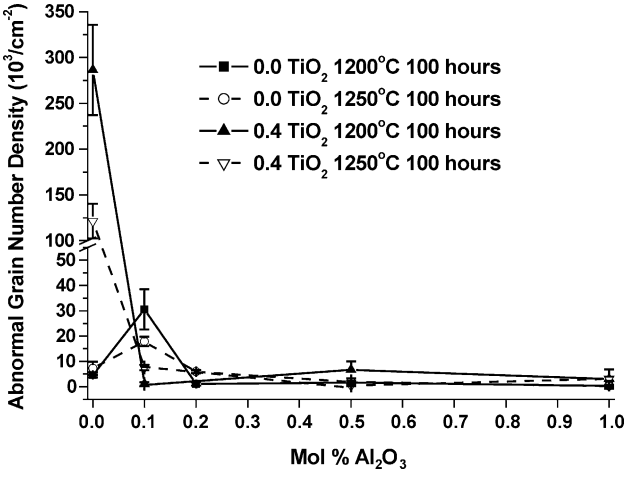

Fig. 4. Abnormal grain number density of $BaTiO_3$–x mol% Al_2O_3 and $BaTiO_3$–0.4 mol% TiO_2–x mol% Al_2O_3 samples sintered at 1200 and 1250 °C for 100 h.

Another amorphous pocket from a series A sample doped with 0.1 mol% Al_2O_3 is shown in Fig. 6(a). Fig. 6(b) shows an amorphous pocket at a multi-grain junction in an A series sample doped with 1 mol% Al_2O_3. The selected area diffraction pattern (SADP) of the amorphous pocket is shown in the inset. Rings showing the presence of an amorphous phase are clearly seen. Diffraction spots from the surrounding grains are also visible. The amorphous phase indicates that a liquid phase was present during sintering. The presence of a liquid phase at a sintering temperature of 1250 °C is not expected from the compatibility phase diagram[29] but the presence of SiO_2 impurity in the $BaTiO_3$ powder has lowered the eutectic temperature to ~1250 °C.[9]

In both these samples the amorphous phase does not appear to have wetted the grain boundaries, as typically shown in the insert in Fig. 6(a). It is possible that the liquid phase wetted the grain boundaries during sintering and then dewetted during cooling of the samples. Choi et al.[30] found similar liquid pockets at triple junctions between matrix grains in TiO_2-excess $BaTiO_3$ sintered at 1350 °C. They also found that if grain growth could be suppressed (in their case by pretreatment of the samples in H_2 at 1250 °C), this liquid did

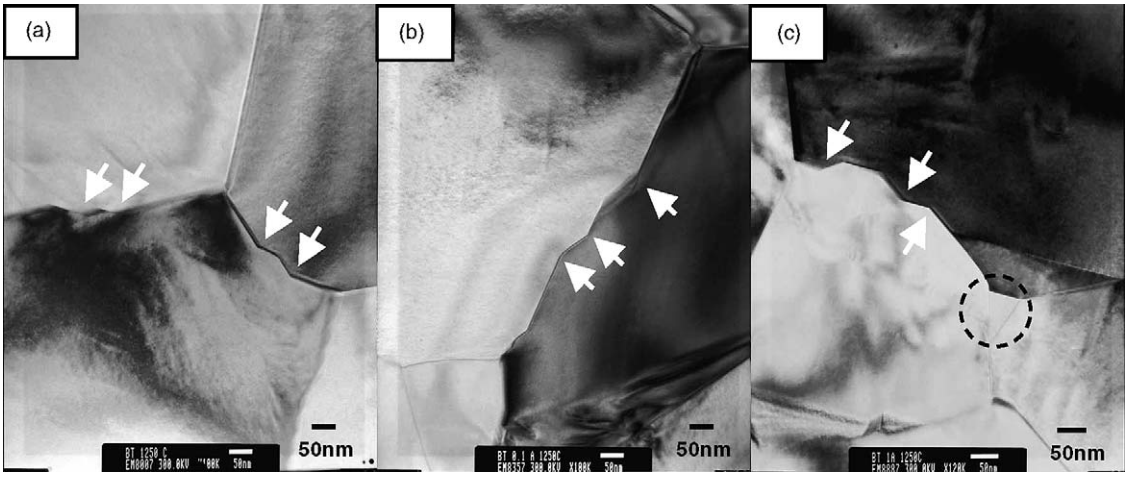

Fig. 5. TEM micrographs of: (a) 0; (b) 0.1 and (c) 1.0 mol% Al_2O_3-doped samples sintered at 1250 °C for 100 h.

not penetrate the grain boundaries even after prolonged sintering at 1350 °C. Moreover, they found that if abnormal grain growth and grain boundary wetting did take place, the liquid phase remained at the grain boundary and did not dewet upon cooling. In the present work, the liquid phase is also found at the triple junctions of matrix grains. These grains have undergone very limited grain growth and so it is likely that grain boundary wetting has not taken place. Plus, if a liquid phase had wetted the grain boundaries during sintering, it would be expected to remain at the grain boundaries during cooling, as shown in the work of Choi et al.[30]

Fig. 7 shows SEM micrographs of the samples. Fig. 7(a) shows a series T sample without Al_2O_3 doping that was sintered at 1200 °C for 100 h. Matrix grains, elongated abnormal grains and a second phase (marked with an arrow) are present. WDS of this second phase identifies it as $Ba_6Ti_{17}O_{40}$. Fig. 7(b) shows a series A sample doped with 0.5 mol% Al_2O_3 that was sintered at 1200 °C for 100 h. Elongated abnormal grains containing {1 1 1} twins are present. Precipitates of a second phase (marked by arrows) are present both in abnormal grains and in the matrix. Precipitates appear in the series A samples when >0.1 mol% Al_2O_3 is added. WDS analysis of this second phase gives it a Ba/Al/Ti cation ratio close to 3/1/6. However, a compound with this cation ratio does not appear on the compatibility diagram of the $BaO–Al_2O_3–TiO_2$ system, the closest phase being

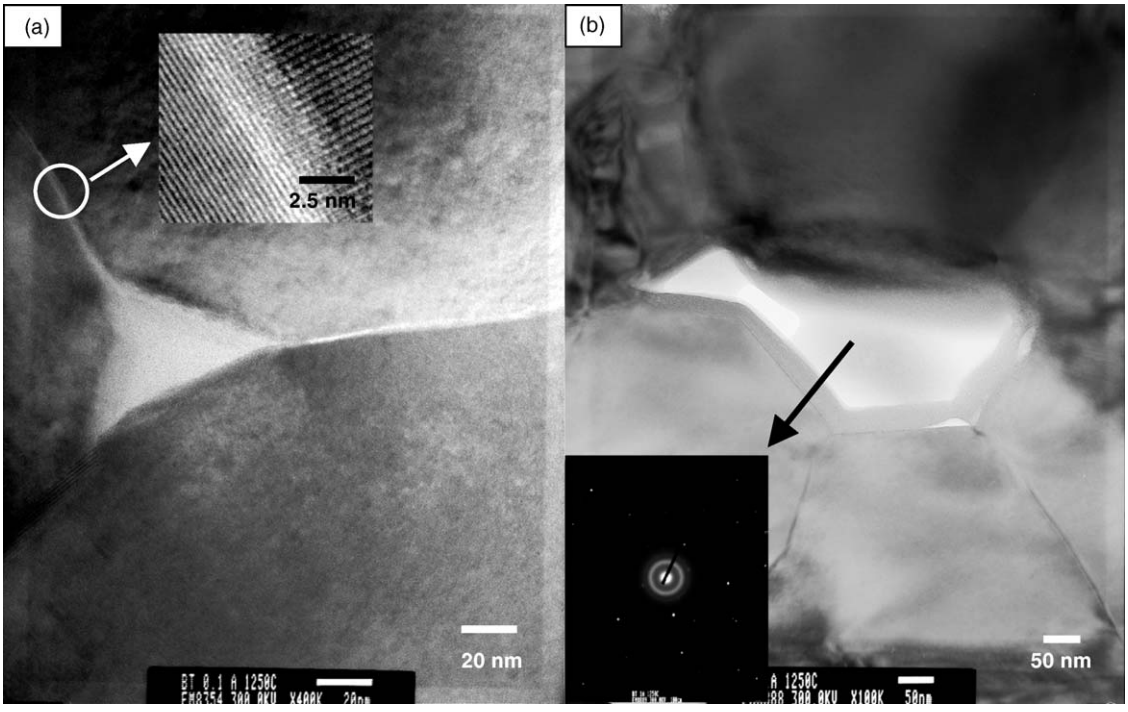

Fig. 6. TEM micrographs of amorphous phases in: (a) 0.1 and (b) 1.0 Al_2O_3-doped samples sintered at 1250 °C for 100 h.

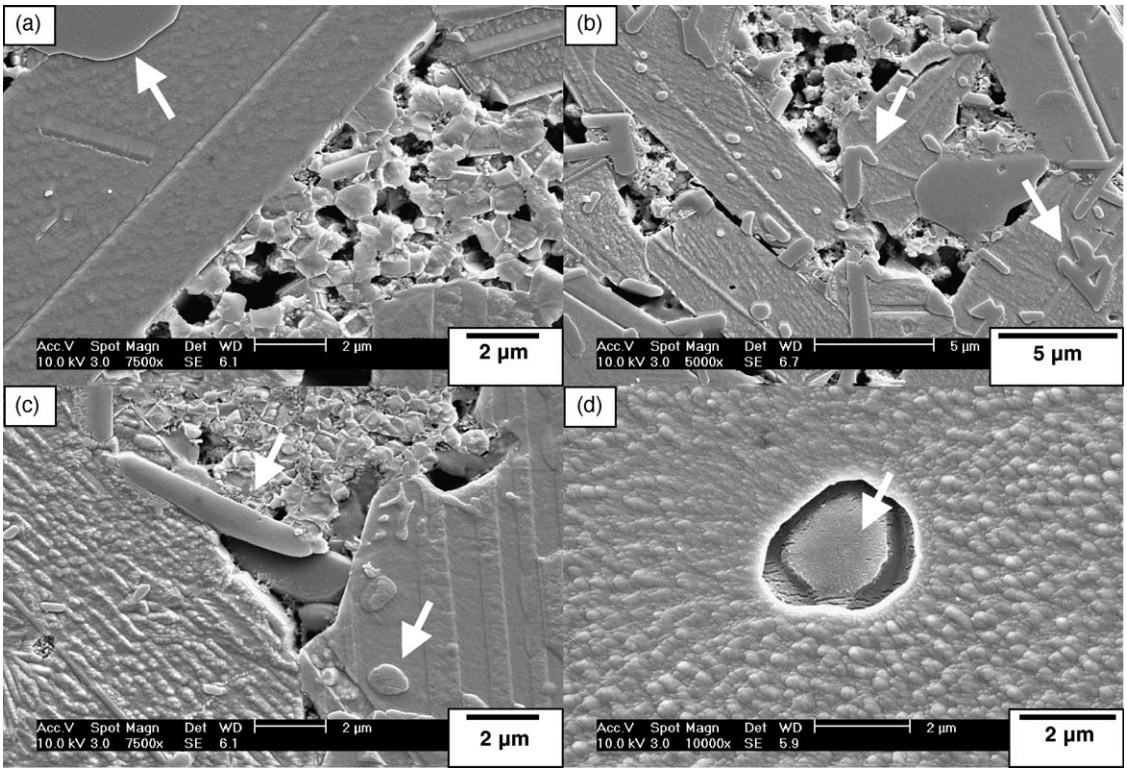

Fig. 7. SEM micrographs of: (a) 0.4 TiO_2-doped sample sintered at 1200 °C for 100 h; (b) 0.5 Al_2O_3-doped sample sintered at 1200 °C for 100 h; (c) 0.4 TiO_2–0.1 Al_2O_3-doped sample sintered at 1200 °C for 100 h; (d) 0.4 TiO_2–0.5 Al_2O_3-doped sample sintered at 1250 °C for 10 h.

$Ba_4Al_2Ti_{10}O_{27}$.[29] The compositions sintered in this work lie on the border of the $BaTiO_3$–$Ba_6Ti_{17}O_{40}$–$Ba_4Al_2Ti_{10}O_{27}$ and $BaTiO_3$–$Ba_4Al_2Ti_{10}O_{27}$–$BaAl_2O_4$ compatibility triangles so this second phase is likely to be $Ba_4Al_2Ti_{10}O_{27}$. In the series T samples, precipitates of the same composition appear in the samples as soon as Al_2O_3 is added (Fig. 7(c)). Precipitates with the composition $BaAl_2O_4$ also appear in the series A and series T samples doped with >0.1 mol% Al_2O_3 (Fig. 7(d)). These $BaAl_2O_4$ precipitates appear both in the abnormal grains and in the matrix. These $Ba_4Al_2Ti_{10}O_{27}$ and $BaAl_2O_4$ precipitates appear in samples sintered at both 1200 and 1250 °C.

TEM micrographs of precipitates are shown in Fig. 8. Fig. 8(a) shows a barium aluminotitanate precipitate. The selected area diffraction pattern for this precipitate is shown in Fig. 8(c). This precipitate has a composition close to $BaAl_2Ti_5O_{14}$ as measured by energy dispersive spectroscopy (EDS). However, due to the overlap of the Ba Lα and Ti Kα peaks, it is not possible to accurately measure the composition of barium titanate phases using EDS. Given the position of the compositions on the subsolidus compatibility diagram of the BaO–Al_2O_3–TiO_2 system[29] and the previous WDS results this phase is likely to be $Ba_4Al_2Ti_{10}O_{27}$. Fig. 8(b) shows a barium aluminate precipitate of composition (as measured by EDS) $BaAl_2O_4$. The selected area diffraction pattern for this precipitate is shown in Fig. 8(d). The $Ba_4Al_2Ti_{10}O_{27}$ precipitate has a rod morphology. The $BaAl_2O_4$ precipitate has an irregular morphology. Both precipitates have smooth (atomically rough) grain boundaries with the surrounding matrix grains.

The undoped series A sample has a mean matrix grain size of 1.3 μm as measured by SEM. The undoped series T sample has a mean matrix grain size of 0.8 μm. Additions of Al_2O_3 cause the matrix grain size to decrease in both series of samples, with the grain size levelling out at 0.5–0.7 μm with addition of 0.5 mol% Al_2O_3. The matrix grain size is not greatly affected by the sintering temperature. The reduction in matrix grain size when Al_2O_3 or TiO_2 is added may be due to solute segregation at the grain boundaries. Acceptor dopants are known to segregate at grain boundaries in $BaTiO_3$.[31] Sharma et al.[32] found the solubility of TiO_2 in $BaTiO_3$ to be <0.1 mol%. Lee et al.[33] have shown that TiO_2 segregates to the grain boundaries in 0.2 mol% excess TiO_2–$BaTiO_3$ during sintering at 1250 °C. Segregation of dopants at the grain boundaries may impede grain growth by the solute drag mechanism.[34,35]

4. Discussion

The presence of abnormal grains and faceted matrix grains (Figs. 1–3 and 5) suggests that grain growth in the samples has taken place by an interface reaction-controlled mechanism.[6,36–40] In this mechanism, grain growth rate is negligible below a critical driving force and increases rapidly above the critical driving force. Therefore, only matrix grains

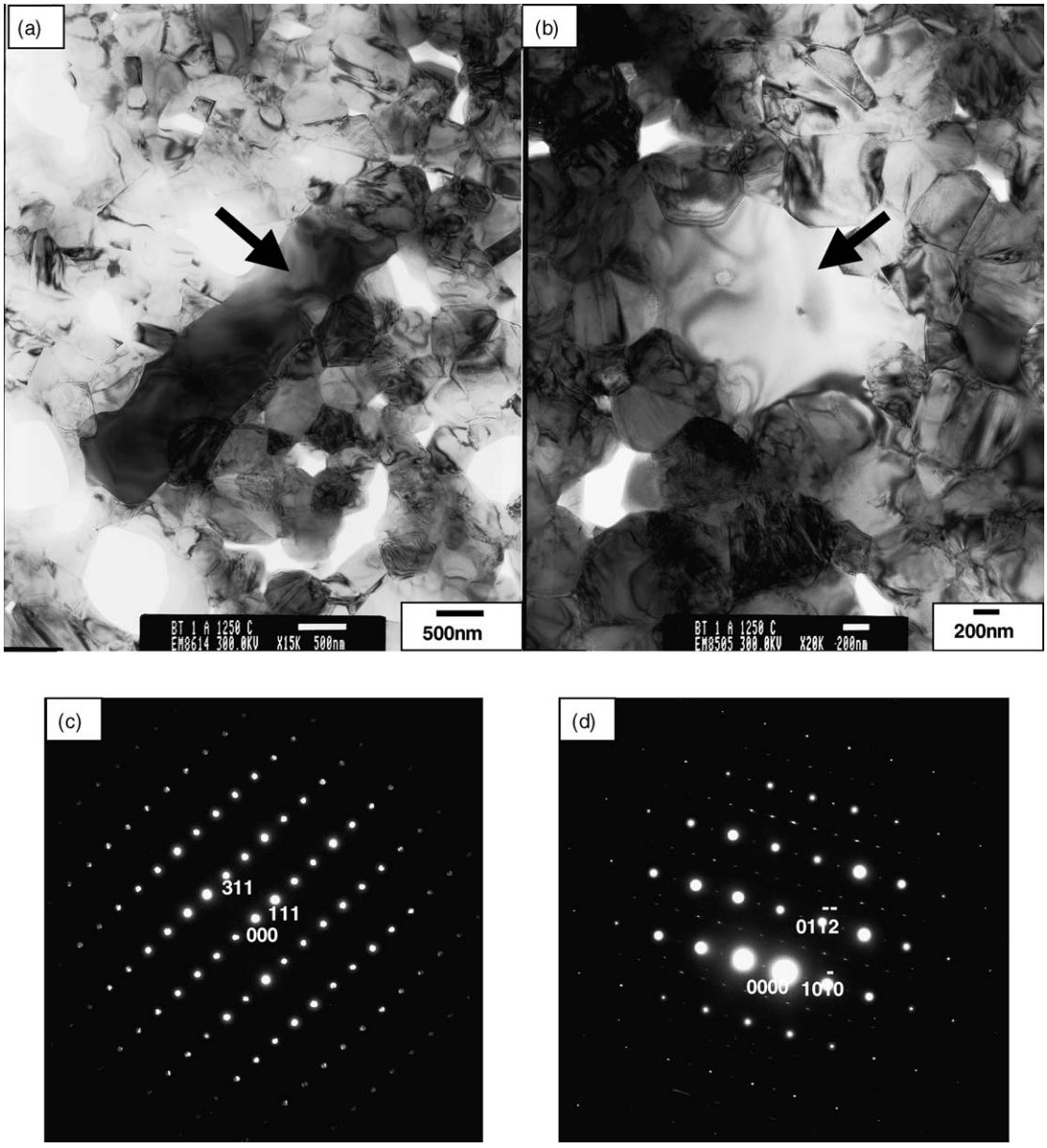

Fig. 8. TEM micrographs of: (a) $Ba_4Al_2Ti_{10}O_{27}$ and (b) $BaAl_2O_4$ precipitates in a 1.0 mol% Al_2O_3-doped sample sintered at 1250 °C for 100 h. (c) and (d) are SADPs of the $Ba_4Al_2Ti_{10}O_{27}$ and $BaAl_2O_4$ precipitates, respectively.

above a certain critical size may grow, but they may do so very rapidly. In the particular case of $BaTiO_3$, $\{1\,1\,1\}$ twins provide low-energy sites for 2D nucleation which are necessary for AGG in samples sintered at temperatures $\leq$1250 °C.[5,6,14,15] This leads to a bimodal structure of very fine matrix grains and coarse abnormal grains containing $\{1\,1\,1\}$ twins.

The effect of Al_2O_3 on abnormal grain growth in $BaTiO_3$ can be explained by the presence of the second phases visible in the SEM and TEM micrographs and by considering the subsolidus compatibility diagram of the $BaO–Al_2O_3–TiO_2$ system.[29] The compositions sintered in this work lie on the border of the $BaTiO_3–Ba_6Ti_{17}O_{40}–Ba_4Al_2Ti_{10}O_{27}$ and $BaTiO_3–Ba_4Al_2Ti_{10}O_{27}–BaAl_2O_4$ compatibility triangles. The $BaTiO_3$ powder used in this work had a slight excess of Ti (Table 1). This excess Ti reacts with $BaTiO_3$ during sintering to form $Ba_6Ti_{17}O_{40}$,[1] which acts as a site for the nucleation of $\{1\,1\,1\}$ double twins.[13,16] These twins in turn provide non-vanishing sites for abnormal grain growth.[5,14,15] This is why the series A samples with 0 mol% Al_2O_3 exhibit AGG.

When Al_2O_3 is added to $BaTiO_3$ it can enter into solid solution according to the reaction:

$$BaTiO_3 + xAl_2O_3 \rightarrow Ba(Ti_{1-2x}Al_{2x})O_{3-x} + 2xTiO_2.$$

When 0.1 mol% Al_2O_3 is added it appears that it is all able to enter into solid solution with $BaTiO_3$, as shown by the absence of Al_2O_3-containing second phases in the SEM

micrographs. This releases TiO_2, which can then react with $BaTiO_3$ to form $Ba_6Ti_{17}O_{40}$. This causes an increase in the number of abnormal grains. When >0.1 mol% Al_2O_3 is added, it does not completely enter into solid solution. The free Al_2O_3 can then react with $BaTiO_3$, $Ba_6Ti_{17}O_{40}$ and the TiO_2 released from $BaTiO_3$ by solid solution of Al_2O_3. The sample composition moves into the $BaTiO_3$–$Ba_4Al_2Ti_{10}O_{27}$–$BaAl_2O_4$ compatibility triangle and the amount of $Ba_6Ti_{17}O_{40}$ is reduced. $Ba_4Al_2Ti_{10}O_{27}$ and $BaAl_2O_4$ precipitates have atomically rough grain boundaries (Fig. 8) and so do not act as sites for formation of {1 1 1} twins.[15,16] Therefore, they cannot act as sites for abnormal grain growth. The removal of $Ba_6Ti_{17}O_{40}$ causes the decrease in the number of abnormal grains. The Al_2O_3 effectively scavenges excess TiO_2 from the grain boundaries. Similar behaviour has been observed in Na_2O-[21] and La_2O_3-doped $BaTiO_3$[11] through the formation of Na_4TiO_4 and $La_2Ti_2O_7$ second phases, respectively.

In the T series samples with no added Al_2O_3, the number of abnormal grains is much greater than in the corresponding A series samples. Such behaviour has previously been observed in $BaTiO_3$[41] and is due to the 0.4 mol% excess TiO_2. This excess TiO_2 reacts with $BaTiO_3$ during sintering to form $Ba_6Ti_{17}O_{40}$, which promotes AGG as described above. During sintering of the T series samples with added Al_2O_3, rather than enter into solid solution in $BaTiO_3$, Al_2O_3 is able to react with the excess TiO_2 and with $BaTiO_3$ to form $Ba_4Al_2Ti_{10}O_{27}$ and $BaAl_2O_4$ precipitates. This prevents the excess TiO_2 from forming $Ba_6Ti_{17}O_{40}$ and accounts for the immediate drop in AGG when 0.1 mol% Al_2O_3 is added. The change in shape of the abnormal grains from elongated to polyhedral in the samples sintered at 1250 °C also indicates that the excess TiO_2 is being scavenged. Cho et al.[17] found that the grain shape of abnormal grains in $BaTiO_3$ samples sintered at 1250 °C changed from elongated to polyhedral as the excess Ti fraction decreased from 0.5 to 0.3 at.%. This was due to a change in the stable grain boundaries of the abnormal grains from {1 1 1} boundaries to {1 0 0} boundaries.

The AGG behaviour of two of the compositions sintered at 1200 °C is unusual. The A series sample doped with 0.1 mol% Al_2O_3 and the T series sample without Al_2O_3 doping both have a higher abnormal grain number density when sintered at 1200 °C than when sintered at 1250 °C (Fig. 4). One would expect this behaviour to be the other way around because the critical driving force for grain growth should increase with sintering temperature decrease.[37,39] There are two possible reasons for this behaviour. The first is that the solubility of Ti in $BaTiO_3$ has increased with sintering temperature. This will remove excess Ti and $Ba_6Ti_{17}O_{40}$ from the grain boundaries and reduce AGG. The second possibility is that grain coalescence is taking place in the samples sintered at 1250 °C with the larger abnormal grains consuming the smaller abnormal grains. The abnormal grains in the samples sintered at 1250 °C are much larger than those in the samples sintered at 1200 °C, indicating that coalescence may have occurred. On the other hand, measurements of abnormal grain number density of samples of these two compositions sintered at 1250 °C for 10 h show the number density to be similar to that of the samples sintered for 100 h. This indicates that coalescence has either not taken place or has taken place at sintering times <10 h. Therefore, we cannot be certain of the reason for this unusual AGG behaviour at this time.

From the results it can be seen that addition of Al_2O_3 can have a significant effect on abnormal grain growth in $BaTiO_3$ samples sintered at temperatures ≤1250 °C. The effect that Al_2O_3 has on AGG is dependant on the amount of excess TiO_2 present in the samples. When no excess TiO_2 is present, addition of Al_2O_3 can cause an increase or a decrease in the amount of abnormal grain growth, depending on the amount of Al_2O_3 added and the types of second phase formed. When TiO_2 is added deliberately, addition of Al_2O_3 effectively suppresses abnormal grain growth as a result of the formation of second phases, which do not act as nucleation sites for {1 1 1} twins.

5. Conclusions

$BaTiO_3$ has been doped with up to 1 mol% Al_2O_3 and sintered at temperatures ≤1250 °C. Samples with and without additions of 0.4 mol% TiO_2 were sintered. In the samples doped with Al_2O_3 alone, addition of up to 0.1 mol% Al_2O_3 promoted abnormal grain growth, while further additions of Al_2O_3 inhibited it. Promotion of abnormal grain growth is caused by Al_2O_3 dissolving in the $BaTiO_3$ lattice and releasing TiO_2. This excess TiO_2 reacts with $BaTiO_3$ to form $Ba_6Ti_{17}O_{40}$, which acts as a nucleation site for {1 1 1} twins. These twins in turn act as low energy growth sites for abnormal grains. On further addition of Al_2O_3, inhibition of abnormal grain growth occurs by Al_2O_3 reacting with $BaTiO_3$, $Ba_6Ti_{17}O_{40}$ and excess TiO_2 to form $Ba_4Al_2Ti_{10}O_{27}$ and $BaAl_2O_4$. Neither of these second phases have faceted grain boundaries, and so cannot form nucleation sites for {1 1 1} twins. Hence they do not act as growth sites for abnormal grains. In the samples doped with Al_2O_3 and TiO_2, addition of Al_2O_3 immediately causes a decrease in abnormal grain growth. This is due to the Al_2O_3 reacting with the excess TiO_2 and $BaTiO_3$ to form $Ba_4Al_2Ti_{10}O_{27}$ and $BaAl_2O_4$, thus preventing the formation of $Ba_6Ti_{17}O_{40}$ by the excess TiO_2.

Acknowledgements

This work was supported by the Korean Ministry of Education under the BK21 program. The authors would like to thank Seon-Young Lee, Song-Sun Bae and Eun-Kyung Lim for operating the SEM, WDS and TEM, respectively.

References

1. Kirby, K. W. and Wechsler, B. A., Phase relations in the barium titanate–titanium oxide system. *J. Am. Ceram. Soc.*, 1991, **74**(8), 1841–1847.

2. Lin, T. F., Hu, C. T. and Lin, I. N., Influence of stoichiometry on the microstructure and positive temperature coeffiecient of resistivity of semiconducting barium titanate ceramics. *J. Am. Ceram. Soc.*, 1990, **73**(3), 531–536.
3. Hennings, D. F. K., Janssen, R. and Reynen, P. J. L., Control of liquid-phase-enhanced discontinuous grain growth in barium titanate. *J. Am. Ceram. Soc.*, 1987, **70**(1), 23–27.
4. Lee, H. Y., Kim, J. S., Hwang, N. M. and Kim, D. Y., Effect of sintering temperature on the secondary abnormal grain growth of $BaTiO_3$. *J. Eur. Ceram. Soc.*, 2000, **20**, 731–737.
5. Lee, H. Y., Kim, J. S. and Kim, D. Y., Effect of twin-plane reentrant edge on the coarsening behaviour of barium titanate grains. *J. Am. Ceram. Soc.*, 2002, **85**(4), 977–980.
6. Lee, B. K., Chung, S. Y. and Kang, S.-J. L., Grain boundary faceting and abnormal grain growth in $BaTiO_3$. *Acta Mater.*, 2000, **48**, 1575–1589.
7. Lin, M. H., Chou, J. F. and Lu, H. Y., The rate-determining mechanism in the sintering of undoped nonstoichiometric barium titanate. *J. Eur. Ceram. Soc.*, 2000, **20**, 517–526.
8. Jung, Y. I., Choi, S. Y. and Kang, S.-J. L., Grain-growth behaviour during stepwise sintering of barium titanate in hydrogen gas and air. *J. Am. Ceram. Soc.*, 2003, **86**(12), 2228–2230.
9. Matsuo, Y. and Sasaki, H., Exaggerated grain growth in liquid-phase sintering of $BaTiO_3$. *J. Am. Ceram. Soc.*, 1971, **52**(9), 471.
10. Daniels, J., Hardlt, K. H. and Wernicke, R., The PTC effect of barium titanate. *Philips Tech. Rev.*, 1978/79, **38**(3), 73–82.
11. Lin, M. H. and Lu, H. Y., Densification retardation in the sintering of La_2O_3-doped barium titanate ceramic. *Mater. Sci. Eng. A*, 2002, **323**, 167–176.
12. Peng, C. J. and Lu, H. Y., Compensation effect in semiconducting barium titanate. *J. Am. Ceram. Soc.*, 1988, **71**(1), C44–C46.
13. Lee, B. K. and Kang, S.-J. L., Second-phase assisted formation of $\{1\,1\,1\}$ twins in barium titanate. *Acta Mater.*, 2001, **49**, 1373–1381.
14. Schmelz, H. and Meyer, A., The evidence for anomalous grain growth below the eutectic temperature in $BaTiO_3$ ceramics. *Ceram. Forum Int., Ber. Dtsch. Keram. Ges.*, 1982, **59**(8), 436–440.
15. Lee, B. K., Jung, Y. I., Kang, S.-J. L. and Nowotny, J., $\{1\,1\,1\}$ twin formation and abnormal grain growth in barium strontium titanate. *J. Am. Ceram. Soc.*, 2003, **86**(1), 155–160.
16. Jung, Y. I., Lee, B. K. and Kang, S.-J. L., Effect of $Ba_6Ti_{17}O_{40}/BaTiO_3$ interface structure on $\{1\,1\,1\}$ twin formation and abnormal grain growth in $BaTiO_3$. *J. Am. Ceram. Soc.*, 2004, **87**(4), 739–741.
17. Cho, Y. K., Kang, S.-J. L. and Yoon, D. Y., Dependance of grain growth and grain-boundary structure on the Ba/Ti ratio in $BaTiO_3$. *J. Am. Ceram. Soc.*, 2004, **87**(1), 119–124.
18. Caballero, A. C., Fernández, J. F., Moure, C., Durán, P. and Chiang, Y. M., Grain growth control and dopant distribution in ZnO-doped $BaTiO_3$. *J. Am. Ceram. Soc.*, 1998, **81**(4), 939–944.
19. Xue, J., Li, C., Zhao, M., Ni, H. and Yin, Z., Studies on the preparation of positive temperature coefficient of resistivity powder by two chemical steps. *J. Mater. Sci.*, 1997, **32**, 6095–6099.
20. Huybrechts, B., Ishizaki, K. and Takata, M., Influence of high oxygen partial pressure annealing on the positive temperature coefficient of Mn-doped $Ba_{0.8}Sr_{0.2}TiO_3$. *J. Eur. Ceram. Soc.*, 1993, **11**, 395–400.
21. Lin, M. H., Chou, J. F. and Lu, H. Y., Grain-growth inhibition in Na_2O-doped TiO_2-excess barium titanate ceramic. *J. Am. Ceram. Soc.*, 2000, **83**(9), 2155–2162.
22. Čeh, M. and Kolar, D., Solubility of calcium oxide in barium titanate. *Mater. Res. Bull.*, 1994, **29**(3), 269–275.
23. Kutty, T. R. N. and Hari, N. S., Effect of charge redistribution through secondary phase formation on PTCR characteristics of n-$BaTiO_3$ ceramics. *Mater. Lett.*, 1998, **34**, 43–49.
24. Al-Allak, H. M., Parry, T. V., Russell, G. J. and Woods, J., Effects of aluminium on the electrical and mechanical properties of PTCR $BaTiO_3$ ceramics as a function of the sintering temperature. *J. Mater. Sci.*, 1988, **23**, 1083–1089.
25. Matsuo, Y., Fujimura, M., Sasaki, H., Nagase, K. and Hayakawa, S., Semiconducting $BaTiO_3$ with additions of Al_2O_3, SiO_2 and TiO_2. *Bull. Am. Ceram. Soc.*, 1968, **47**(3), 292–297.
26. Cheng, H. F., Effect of sintering aids on the electrical properties of positive temperature coefficient of resistivity $BaTiO_3$ ceramics. *J. Appl. Phys.*, 1989, **66**(3), 1382–1387.
27. Schatt, W. and Wieters, K. P., *Powder Metallurgy*. European Powder Metallurgy Association, UK, 1997.
28. DeVries, R. C., Lowering of Curie temperature of $BaTiO_3$ by chemical reduction. *J. Am. Ceram. Soc.*, 1960, **43**, 226.
29. Roth, R. S., Brower, W. S., Austin, M. and Koob, M., *Phase Diagrams for Ceramists*, *Vol 6*, ed. R. S. Roth, J. R. Dennis and H. F. McMurdie. The American Ceramic Society, OH, 1987, p. 271.
30. Choi, S. Y., Yoon, D. Y. and Kang, S.-J. L., Kinetic formation and thickening of intergranular amorphous films at grin boundaries in barium titanate. *Acta Mater.*, 2004, **52**, 3721–3726.
31. Chiang, Y. M. and Takagi, T., Grain-boundary chemistry of barium titanate and strontium titanate: I. High-temperature equilibrium space charge. *J. Am. Ceram. Soc.*, 1990, **73**(11), 3278–3285.
32. Sharma, R. K., Chan, N. H. and Smyth, D. M., Solubility of TiO_2 in $BaTiO_3$. *J. Am. Ceram. Soc.*, 1981, **64**(8), 448–451.
33. Lee, S. B., Sigle, W. and Rühle, M., Investigation of grain boundaries in abnormal grain growth structure of TiO_2-excess $BaTiO_3$ by TEM and EELS analysis. *Acta Mater.*, 2002, **50**, 2151–2162.
34. Powers, J. D. and Glaeser, A. M., Grain boundary migration in ceramics. *Interf. Sci.*, 1998, **6**(1), 23–29.
35. Chung, S. Y., Kang, S.-J. L. and Dravid, V. P., Effect of sintering atmosphere on grain boundary segregation and grain growth in niobium-doped $SrTiO_3$. *J. Am. Ceram. Soc.*, 2002, **85**(11), 2805–2810.
36. Gleiter, H., The mechanism of grain boundary migration. *Acta Metall.*, 1969, **17**, 565–573.
37. Yoon, D. Y., Park, C. W. and Koo, J. B., The step growth hypothesis for abnormal grain growth. In *Ceramic Interfaces 2*, ed. H. I. Yoo and S.-J. L. Kang. The Institute of Materials, London, UK, 2001.
38. Merkle, K. L., Thompson, L. J. and Phillipp, F., High-resolution electron microscopy of grain boundary migration. *Mater. Res. Soc. Symp. Proc.*, 2001, **652**, Y2.4.1–Y2.4.11.
39. Koo, J. B. and Yoon, D. Y., Abnormal grain growth in bulk Cu—the dependence on initial grain size and annealing temperature. *Metall. Mater. Trans. A*, 2001, **32**, 1911–1926.
40. Hirth, J. P. and Pound, G. M., *Condensation and Evaporation*. Pergamon Press, Oxford, 1963, p. 77.
41. Lee, B. K., Chung, S. Y. and Kang, S.-J. L., Necessary conditions for the formation of $\{1\,1\,1\}$ twins in barium titanate. *J. Am. Ceram. Soc.*, 2000, **83**(11), 2858–2860.